ELSEVIER

Biophysical Chemistry 104 (2003) 271–278

Biophysical Chemistry

www.elsevier.com/locate/bpc

Cooperative adhesion of ligand–receptor bonds

Xiaohui Zhang*, Vincent T. Moy

Department of Physiology and Biophysics, University of Miami School of Medicine, 1600 N.W. 10th Avenue, Miami, FL 33136, USA

Received 18 August 2002; received in revised form 20 November 2002; accepted 28 November 2002

Abstract

Cooperative (simultaneous) breakage of multiple adhesive bonds has been proposed as a mechanism for enhanced binding strength between adhesion molecules on apposing cell surfaces. In this report, we used the atomic force microscopy (AFM) to study how changes in binding affinity and separation rate of force-induced ligand–receptor dissociation affect binding cooperativity. The AFM force measurements were carried out using (strept)avidin-functionalized cantilever tips and biotinylated agarose beads under conditions where multiple (strept)avidin–biotin linkages were formed following surface contact. At slow surface separation of the AFM cantilever from the bead's surface, the (strept)avidin–biotin linkages appeared to rupture sequentially. Increasing the separation rate from 210 to 1950 nm/s led to a linear increase in the average rupture force. Moreover, force histograms revealed a quantized force distribution that shifted toward higher values with increasing separation rate. In measurements of streptavidin–iminobiotin adhesion, the force distribution also shifted toward higher values when the buffer was adjusted to a higher pH to raise the binding affinity. Together, these results demonstrate that the cooperativity of ligand–receptor bonds is significantly enhanced by increases in surface separation rate and/or binding affinity.

Keywords: Atomic force microscopy; Ligand–receptor interaction; Bond rupture; Adhesion; Single molecule interaction

1. Introduction

Dynamic changes in cell detachment force are critical in development, differentiation, and inflammation [1,2]. Aberrations in cell adhesion mechanisms can lead to uncontrolled cell division and/or transformation of cancerous cells into a metastatic phenotype [3]. The molecular determinants of cell migration and cell–cell adhesion are surface receptors that include members of the integrin, selectin, and immunoglobulin superfamily [4–6]. Mechanisms for enhanced cell adhesion include changes in receptor expression, affinity modulation of receptor, and receptor aggregation [7,8]. Receptor affinity modulation may elevate the activation energy for the dissociation of the adhesion complex, while receptor aggregation may increase the cooperativity of molecular adhesion [9].

Cell adhesion is ultimately governed by the dynamic response of the interacting adhesion mol-

*Corresponding author. Tel.: +1-305-243-3201; fax: +1-305-243-5931.

E-mail addresses:
xzhang@newssun.med.miami.edu (X. Zhang),
vmoy@newssun.med.miami.edu (V.T. Moy).

0301-4622/03/$ - see front matter © 2003 Elsevier Science B.V. All rights reserved.
doi:10.1016/S0301-4622(02)00381-2

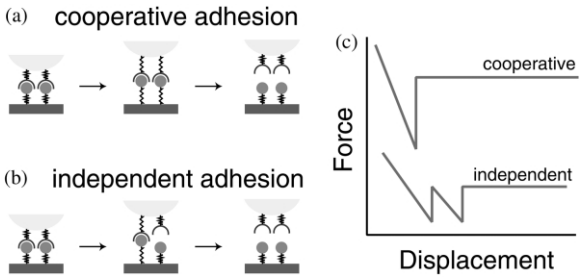

Fig. 1. Schematic of possible mechanisms for surface detachment. (a) In cooperative molecular adhesion multiple ligand–receptor bonds break simultaneously for a large detachment force. (b) During independent molecular adhesion, bonds rupture sequentially and the detachment force is lower. The usage of the term 'cooperative adhesion' here refers to the simultaneous breakage of multiple bonds and not to a change in receptor binding affinity. (c) Diagrammatic force vs. displacement traces of cooperative and independent unbinding of multiple complexes.

ecules to a pulling force [10,11]. The conceptual framework for understanding the forced unbinding of an adhesion complex was formulated by Bell and refined by Evans and others [12,13]. In the Bell model, the applied force lowers the activation energy barrier and thus accelerates the bond dissociation. Although several recent studies have examined the dynamic response of individual complexes [14–18], the effect of an applied force on receptor group dynamics is less well understood.

Since cell adhesion involves the cooperative properties of many bonds, we examined the dynamic response of a system consisting of two bonds anchored by flexible linkers as depicted in Fig. 1. If during surface separation the applied force is distributed unevenly between the bonds, the two bonds will rupture at different times. Alternatively, if the applied force is distributed equally on both bonds, then most likely a larger force will be needed to induce the cooperative dissociation of the bonds. Conditions that favor independent vs. cooperative breakage of ligand–receptor bonds are not well understood.

The interaction between streptavidin and its ligand, biotin, provides an ideal model system for investigating the cooperativity of molecular adhesion. The streptavidin–biotin interaction has been extensively characterized by both biochemical [19] and physical approaches, including atomic force microscopy (AFM), the surface force apparatus and the biomembrane force probe [15,20]. The most prominent feature of the streptavidin–biotin interaction is the high binding affinity. Structurally, this high affinity has been attributed to a network of hydrogen bonds and hydrophobic interactions that stabilize the encapsulated biotin [21–23].

In the current study, we carried out AFM measurements under experimental conditions that would allow for the formation of multiple streptavidin–biotin bonds. The unbinding of the streptavidin–biotin bonds were characterized at different separation rates. In parallel experiments, the streptavidin–iminobiotin system allowed us to examine changes in cooperativity stemming from a change in binding affinity. Our studies revealed that the strength of surface adhesion increases with both binding affinity and surface separation rate as a result of increased cooperativity among ligand–receptor complexes.

2. Material and methods

2.1. Force apparatus

An atomic force apparatus was constructed to acquire force measurements [24]. Cells or agarose beads were localized using an inverted optical system attached to the AFM. The vertical position of the AFM tip relative to the substrate was set by a piezoelectric translator with a strain gauge position sensor (Physik Instrumente, Waldbronn, Germany). The interaction between the AFM tip and the substrate was determined from deflection of the AFM cantilever. A focused laser spot from a pigtail diode laser (Oz Optics, Ontario, Canada) was reflected off the back of the cantilever onto a two-segment photodiode to monitor the cantilever's deflection. The photodiode signal was then preamplified, digitized by a 16-bit analog-to-digital converter (Instrutech Corp., Port Washington, NY), and processed by an Apple Power Macintosh computer. All force scan measurements were recorded at room temperature using unsharpened Si_3N_4 cantilevers (Thermomicroscopes, MLCT-AUHW, Sunnyvale, CA). Cantilevers were calibrated by thermal fluctuation analysis according to

Hutter and Bechhoefer [25] and had a spring constant of approximately 0.010 N/m.

2.2. Functionalization of AFM tips

Cantilevers were coated with biotinylated bovine serum albumin (biotin-BSA) and then coupled with (strept)avidin (streptavidin or Neutravidin) [26]. In brief, cantilevers were washed in acetone for 5 min, UV irradiated for 15 min, and then immersed overnight in 50–100 μl of biotin-BSA (Sigma, St. Louis, MO; 0.5 mg/ml in 100 mM $NaHCO_3$, pH 8.6) in a 37 °C humidified chamber. After several rinses in PBS, biotin-BSA coated tips were then coupled with (strept)avidin (streptavidin, Sigma; Neutravidin, Pierce, Rockford, IL; 0.5 mg/ml in 100 mM $NaHCO_3$) during a 10 min incubation. Unbound (strept)avidin molecules were washed away by several PBS rinses.

2.3. Bead preparation

Cross-linked 4% agarose beads labeled with biotin were obtained from Sigma. Agarose beads were washed 3 times with PBS and resuspended in the same solution for measurements. To minimize bead movement during the force measurements, the biotin-labeled beads were plated on a culture dish coated with streptavidin.

3. Results

The detachment force of streptavidin–biotin-mediated adhesion was measured using an AFM in force scan mode [27]. The AFM cantilevers/tips were functionalized with streptavidin as described in Section 2. At the onset of the force measurement, the streptavidin-functionalized AFM tip was positioned directly above the center of a selected biotin-labeled agarose bead. The tip was lowered onto the bead, while the deflection of the cantilever was measured to obtain the force acting on the system. The maximal indentation force was set at 200 pN and was held constant for 0.25 s. Under these conditions, multiple streptavidin–biotin bonds were always formed following the surface contact. These bonds then gave rise to adhesion between the tip and the bead. The adhesion was quantified by the downward deflection of the cantilever during the retraction of the cantilever/tip from the agarose bead. Records of this cycle are given in Fig. 2. As shown, the retract trace frequently displayed a sawtooth pattern that reflected the complexity of the detachment process. The trace revealed that the surface adhesion was mediated by multiple streptavidin–biotin bonds that did not necessarily rupture simultaneously. Each of the six transitions (rupture events) in Fig. 2a (indicated by arrows) corresponds to the breakage of one or more bonds. The magnitude of these

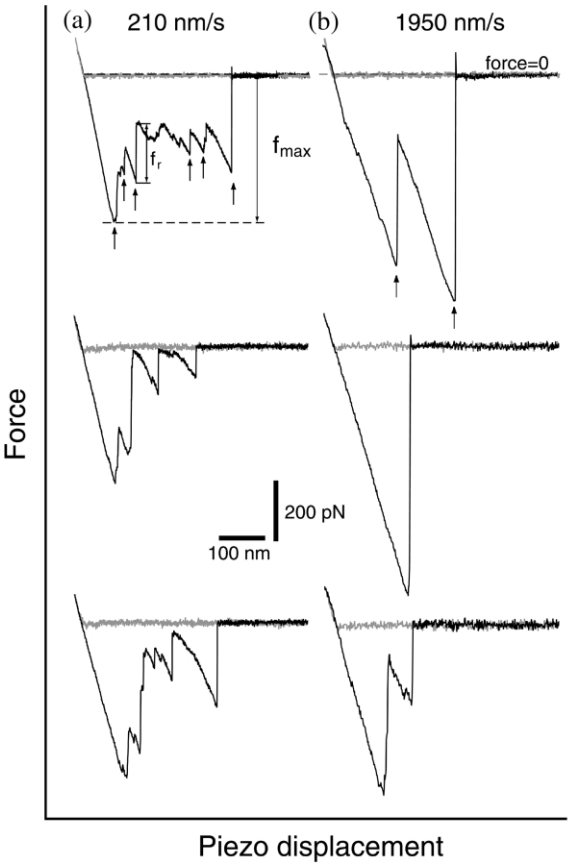

Fig. 2. Series of AFM force scan measurements obtained with surface separation rates of (a) 210 nm/s and (b) 1950 nm/s. The approach traces are shown in gray and the retract traces are shown in black. In the top retract traces, the arrows point to the rupture events, 6 total for (a) and 2 total for (b). In (a), f_{max} is the maximum rupture force. f_r represents the magnitude of one rupture force (the third) of the total 6 rupture events.

transitions is a measure of the applied force f_r needed to rupture the bond(s). As a control, no adhesion was found between the streptavidin-functionalized AFM tip and the biotinylated bead when free streptavidin (50 μg/ml) was present (data not shown).

3.1. Cooperative adhesion and separation rate

To investigate how cooperative adhesion is modulated by the rate of surface separation, force measurements were obtained at different rates of cantilever retraction. Fig. 2 shows a series of force scan measurements obtained at different separation rates: (A) 210 nm/s and (B) 1950 nm/s. The most striking difference between these measurements was (i) higher forces were measured at the faster separation rate and (ii) the number of rupture events was reduced at the faster rate.

The force measurements of the streptavidin–biotin interaction can be characterized by (i) the maximal force reached in a given measurement (f_{max}), (ii) the number of rupture events in a single measurement (N_r), and (iii) the average rupture force of all the rupture events ($\overline{f}_r$) in a single measurement, as indicated in Fig. 2a. To determine how these parameters vary with separation rate, a set of 50 measurements were carried out at different separation rates each between 210 and 1950 nm/s. To permit comparison of the data set, all measurements in a given experiment were obtained with the same AFM cantilever. Fig. 3a and b revealed that both the average force per rupture event and average maximal force increased 2–3-fold over the range of separation rates. In contrast, the average number of rupture events per measurement decreased by a factor of 2 over this range (Fig. 3c). Similar results were observed for the interaction between biotin and avidin, a homologue of streptavidin [19].

It is conceivable that streptavidin or avidin could dissociate from the tip and/or lose its biotin-binding ability during the course of the experiment, resulting in diminished adhesion. A parameter that provides a measure of integrity of the functionalized-AFM tip is the total adhesion force f_T which we defined as the product of the average rupture force and the number of rupture events

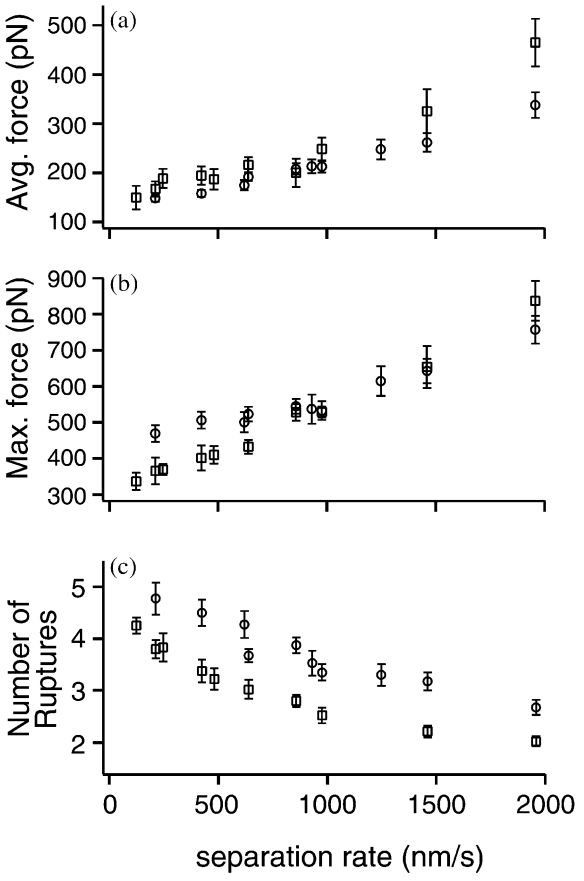

Fig. 3. Separation rate dependence of (strept)avidin–biotin adhesion. (a) Plot of average rupture force vs. separation rate. (b) Plot of average maximum rupture force vs. separation rate. (c) Plot of average number of rupture events vs. separation rate. Square markers correspond to data obtained from the streptavidin–biotin interaction. Circular markers correspond to data obtained from the avidin–biotin interaction. Error bars represent the standard error ($N \geqslant 50$).

(i.e. $f_T = \overline{f}_r \times N_r$) in a single measurement. Although total adhesion depends on several factors, including density of streptavidin on the AFM tip, indentation force, and duration of the tip/bead interaction, it should remain constant in a set of measurements, provided that the experimental conditions are the same and there is no loss in the activity of the functionalized AFM tip. Tip integrity was verified by ensuring f_T remained constant in a given set of measurements. The total adhesion force for the streptavidin ($f_T = 0.799 \pm 0.12$ nN)

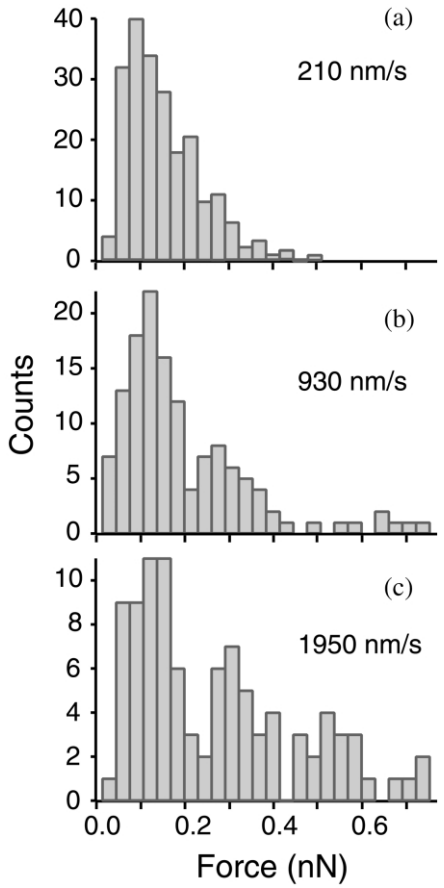

Fig. 4. Force histograms of the streptavidin–biotin interaction obtained at different separation rates: (a) 210 nm/s; (b) 930 nm/s and (c) 1950 nm/s.

and avidin ($f_T = 1.005 \pm 0.086$ nN) measurements summarized in Fig. 3 did not change significantly during the experiments.

Histograms of rupture force at different separation rates were generated from the analysis of the force measurements. Fig. 4 presents force histograms acquired at separation rates of 210, 930 and 1950 nm/s. As shown in Fig. 4a, at a separation rate of 210 nm/s, rupture forces clustered in a single distribution. A second force distribution was evident at a separation rate of 930 nm/s (Fig. 4b). In Fig. 4c, at a separation rate of 1950 nm/s, the rupture forces were clustered approximately 3 peaks. Together with the data presented in Fig. 3, the force histograms revealed that there is a shift toward greater cooperative adhesion with increasing separation rate.

3.2. Cooperative adhesion and binding affinity

To examine the effect of changes in ligand affinity on cooperativity of the receptors, we measured the adhesive strength of the iminobiotin–streptavidin bond. Whereas the interaction between streptavidin and biotin is relatively independent of the pH of the buffer, the binding affinity of iminobiotin and streptavidin increases by approximately four orders of magnitude over the pH range of 6–10 [28]. The variation in the binding affinity constant of the iminobiotin–streptavidin interaction is attributed to the fact that streptavidin binds only to the neutral form of iminobiotin, which has a pK_a of 11.95. The lower binding affinity at lower pH values thus reflects a reduced iminobiotin population that is capable of binding to streptavidin. Thus, the iminobiotin–streptavidin pair provided us with the means to alter binding affinity by simply adjusting the pH of the solution. Fig. 5 summarizes the results of force measurements obtained at pH 6 and 10. In these experiments, force measurements were acquired at pH 6 first, and then NaOH solution was added to the sample chamber to bring the pH of the buffer up to pH 10. After equilibration at pH 10, we acquired force measurements from the same location on the agarose bead. Except for the difference in pH of the buffer, the two sets of measurements were acquired under identical conditions. Fig. 5a plots the average rupture force vs. separation rate. As shown, the average rupture force increased with separation rate at both pH 6 and 10. The increase in rupture force was accompanied by a decrease in the number of rupture events (Fig. 5b). Total rupture force remained constant with changes in separation rates, however, a higher f_T was measured at pH 10 (0.57 ± 0.07 nN) than pH 6 (0.35 ± 0.02 nN). Fig. 6 presents the distribution of rupture forces acquired at a separation rate of 1950 nm/s in pH 6 and 10 buffer. Broad peaks centered at 120, 260 and 380 pN were identifiable in the pH 10 force histogram, whereas only a single broad peak centered at 120 pN was evident in the pH 6 histogram. We attribute the appearance of the additional peaks

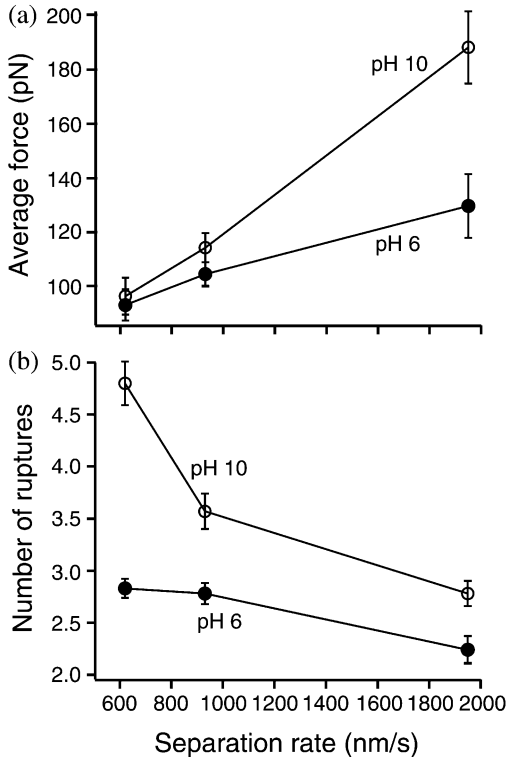

Fig. 5. pH dependence of adhesion between iminobiotin and streptavidin. (a) Plots the average rupture force vs. separation rate. (b) Plots the average number of rupture events per force measurement vs. separation rate. Error bars represent the standard error ($N \geqslant 40$).

in the pH 10 histogram to an increase in cooperative adhesion.

4. Discussion

Although many of the recent studies have focused on the dynamics of individual molecules, it can be argued that the cooperativity among receptors plays a greater role in determining the strength of cell adhesion [15,29]. Fig. 1 depicts two extreme mechanisms for surface detachment: independent and cooperative molecular adhesion. During independent molecular adhesion, bonds rupture sequentially. A sustained force sufficient to rupture a single bond will eventually rupture all of the bonds. In cooperative molecular adhesion, a larger detachment force is needed to rupture the bonds simultaneously (Fig. 1c). In this study, we employed the AFM to investigate the roles of separation rate and affinity modulation in regulating the cooperativity of adhesion complexes. The AFM has sufficient sensitivity and temporal resolution to detect the sequential breakage of individual bonds as demonstrated by Fig. 2. It is also evident that the tip–bead separation does not proceed with the sequential breakage of individual bonds nor does it involve the simultaneous disruption of all the bonds. Instead, it appears that the separation process involves a sequential breakage of cooperative bonds.

In this report, we examined the adhesive properties of receptor-mediated surface interaction as a function of separation rate. The separation rate, together with the spring constants of the cantilever and the agarose filament that linked the biotin to the bead determines the loading rate exerted on the ligand–receptor bonds in the AFM measurements. For the separation rates used in our measurements (210–1950 nm/s), the corresponding loading rates are 1000–10 000 pN/s. Over this range of loading rates, the previously reported rupture force value for the individual streptavidin–

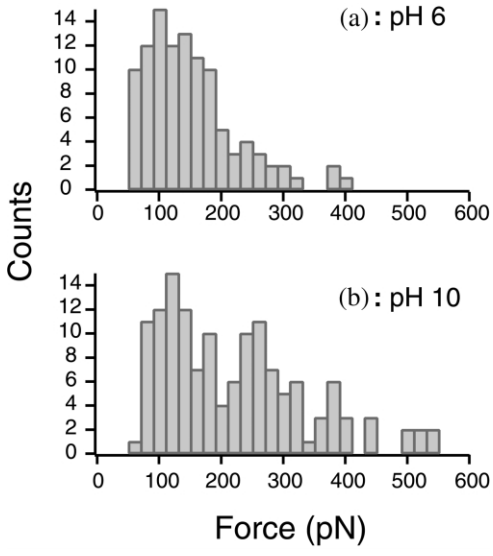

Fig. 6. Histograms of streptavidin–iminobiotin rupture force obtained at (a) pH 6 and (b) pH 10. The separation rate of the measurements was 1950 nm/s.

biotin bond monotonically increases from 70 to 110 pN with increasing loading rate [15]. These force values are consistent with the positions of the first peak in the force histograms of Fig. 4. Hence, we attribute the first peak in each of the force histograms to the breakage of a single streptavidin–biotin complex. A shift in the position of these peaks to higher forces with increasing separation rate is consistent with predictions based on the Bell model. Subsequent peak(s) in Fig. 4b and c are attributed to the simultaneous dissociation of two or more complexes. The appearance of the multiple peaks in the histogram at faster surface separation rates is interpreted as a compelling evidence for molecular cooperativity in adhesion.

Recently the Bell model was extended to consider systems involving multiple bonds under a dynamic load. Seifert showed that the dependence of rupture force on the loading rate can be either linear, like a square root, or logarithmic [30]. Examination of the data in Fig. 3 revealed a linear dependence between force and separation rate, which would suggest that our measurements were carried out in a slow loading rate regime. Although our results are consistent with the theory, there are difficulties with direct comparison of our data with the proposed model. The main problem stemming from the fact that biotin is not coupled to the bead with filaments of equal length, which is not factored into the model.

Enhanced cooperativity can also come about as a result of an increase in binding affinity as demonstrated in the streptavidin–iminobiotin force measurements. A pH dependent increase in binding affinity due to greater cooperativity was evident in Fig. 6 by the appearance of 3 peaks in the pH 10 force histogram. It should be noted that the position of the first peak at $\sim$120 pN remained the same for both pH 6 and 10. This first peak is attributed to the rupture force of a single streptavidin–iminobiotin complex and is independent of binding affinity, as previously reported [29]. Hence, enhanced adhesion as measured by an increase in the average rupture force can be attributed to enhanced cooperativity rather than an increase in the bond strength of the individual ligand–receptor linkage.

Affinity modulation is a common property of integrins [4,31]. For example, the leukocyte integrin, lymphocyte function-associated antigen-1 (LFA-1), mediates the adhesion of T lymphocytes to antigen presenting cells by binding to its ligand, intercellular adhesion molecule-1 (ICAM-1). T lymphocyte activation results in a Mg^{2+} dependent increase in the affinity of the LFA-1/ICAM-1 complex, as well as, a Ca^{2+} dependent clustering of the integrins [32]. The change in binding affinity may or may not result in an increase in the unbinding force of the individual complexes as in the case of the interaction between streptavidin and iminobiotin [29]. If we accept the Bell model, the binding force would scale with the logarithm of the affinity constant (or free energy). The low affinity form of LFA-1 has a K_d of 6.7×10^{-5} M, while high affinity LFA-1 has a K_d of 3.6×10^{-7} M [33]. This 200-fold increase in the binding affinity of LFA-1 translates to a decrease in free energy from -5.7 to -8.8 kcal/mol. If we assume a linear intermolecular potential with an interaction length of 5 Å, the bond strength of low and high affinity forms of the LFA-1/ICAM-1 complex are expected to be 79 and 123 pN, respectively. This is a relatively modest increase in bond strength compared to the increase in total cell adhesion after T cell activation [34]. In this case, an increase in molecular cooperativity may account more for the enhanced cell adhesion than the increase in the bond strength of the individual adhesion complex. Direct force measurements studies such as this one could verify this prediction.

Acknowledgments

We thank A. Chen for insightful discussions and C. Freites for technical support. This work was supported by grants from the American Cancer Society, and the NIH (GM55611) to VTM. XZ receives a predoctoral fellowship from the American Heart Association.

References

[1] J.C. Adams, F.M. Watt, Changes in keratinocyte adhesion during terminal differentiation: reduction in fibro-

nectin binding precedes alpha 5 beta 1 integrin loss from the cell surface, Cell 63 (1990) 425–435.
[2] R. Gonzalez-Amaro, F. Sanchez-Madrid, Cell adhesion molecules: selectins and integrins, Crit. Rev. Immunol. 19 (1999) 389–429.
[3] J. Folkman, A. Moscona, Role of cell shape in growth control, Nature 273 (1978) 345–349.
[4] R.O. Hynes, Integrins: versatility, modulation, and signaling in cell adhesion, Cell 69 (1992) 11–25.
[5] M.B. Lawrence, T.A. Springer, Leukocytes roll on a selectin at physiologic flow rates: distinction from and prerequisite for adhesion through integrins, Cell 65 (1991) 859–873.
[6] T.A. Springer, Adhesion receptors of the immune system, Nature 346 (1990) 425–434.
[7] M.S. Diamond, T.A. Springer, The dynamic regulation of integrin adhesiveness, Curr. Biol. 4 (1994) 506–517.
[8] A. Hermanowski-Vosatka, P.A. Detmers, O. Gotze, S.C. Silverstein, S.D. Wright, Clustering of ligand on the surface of a particle enhances adhesion to receptor-bearing cells, J. Biol. Chem. 263 (1988) 17822–17827.
[9] M.L. Dustin, Making a little affinity go a long way: a topological view of LFA-1 regulation, Cell Adhes. Commun. 6 (1998) 255–262.
[10] R. Alon, S. Chen, K.D. Puri, E.B. Finger, T.A. Springer, The kinetics of L-selectin tethers and the mechanics of selectin-mediated rolling, J. Cell Biol. 138 (1997) 1169–1180.
[11] M.J. Smith, E.L. Berg, M.B. Lawrence, A direct comparison of selectin-mediated transient, adhesive events using high temporal resolution, Biophys. J. 77 (1999) 3371–3383.
[12] G.I. Bell, Models for the specific adhesion of cells to cells, Science 200 (1978) 618–627.
[13] E. Evans, K. Ritchie, Dynamic strength of molecular adhesion bonds, Biophys. J. 72 (1997) 1541–1555.
[14] G.U. Lee, L.A. Chrisey, R.J. Colton, Direct measurement of the forces between complementary strands of DNA, Science 266 (1994) 771–773.
[15] R. Merkel, P. Nassoy, A. Leung, K. Ritchie, E. Evans, Energy landscapes of receptor–ligand bonds explored with dynamic force spectroscopy, Nature 397 (1999) 50–53.
[16] P. Hinterdorfer, W. Baumgartner, H.J. Gruber, K. Schilcher, H. Schindler, Detection and localization of individual antibody–antigen recognition events by atomic force microscopy, Proc. Natl. Acad. Sci. USA 93 (1996) 3477–3481.
[17] T. Strunz, K. Oroszlan, R. Schafer, H.J. Guntherodt, Dynamic force spectroscopy of single DNA molecules, Proc. Natl. Acad. Sci. USA 96 (1999) 11277–11282.
[18] H. Grubmüller, B. Heymann, P. Tavan, Ligand binding: molecular mechanics calculation of the streptavidin–biotin rupture force, Science 271 (1996) 997–999.
[19] N.M. Green, Avidin, Adv. Prot. Chem. 29 (1975) 85–133.
[20] E.L. Florin, V.T. Moy, H.E. Gaub, Adhesion forces between individual ligand–receptor pairs, Science 264 (1994) 415–417.
[21] W.A. Hendrickson, A. Pähler, J.L. Smith, Y. Satow, E.A. Merritt, R.P. Phizackerley, Crystal structure of core streptavidin determined from multiwavelength anomalous diffraction of synchrotron radiation, Proc. Natl. Acad. Sci. USA 86 (1989) 2190–2194.
[22] P.C. Weber, D.H. Ohlendorf, J.J. Wendoloski, F.R. Salemme, Structural origins of the high-affinity biotin binding to streptavidin, Science 243 (1989) 85–88.
[23] D.E. Hyre, L.M. Amon, J.E. Penzotti, et al., Early mechanistic events in biotin dissociation from streptavidin, Nat. Struct. Biol. 9 (2002) 582–585.
[24] C. Yuan, A. Chen, P. Kolb, V.T. Moy, Energy landscape of streptavidin–biotin complexes measured by atomic force microscopy, Biochemistry 39 (2000) 10219–10223.
[25] J.L. Hutter, J. Bechhoefer, Calibration of atomic-force microscope tips, Rev. Sci. Instrum. 64 (1993) 1868–1873.
[26] V.T. Moy, E.-L. Florin, H.E. Gaub, Adhesive forces between ligand and receptor measured by AFM, Colloid. Surface. 93 (1994) 343–348.
[27] N.A. Burnham, R.J. Colton, H.M. Pollock, Interpretation issues in force microscopy, J. Vac. Soc. Technol. A 9 (1991) 2548–2556.
[28] N.M. Green, Thermodynamics of the binding of biotin and some analogues by avidin, Biochem. J. 101 (1966) 774.
[29] V.T. Moy, E.L. Florin, H.E. Gaub, Intermolecular forces and energies between ligands and receptors, Science 266 (1994) 257–259.
[30] U. Seifert, Rupture of multiple parallel molecular bonds under dynamic loading, Phys. Rev. Lett. 84 (2000) 2750–2753.
[31] M.L. Dustin, T.A. Springer, T-cell receptor cross-linking transiently stimulates adhesiveness through LFA-1, Nature 341 (1989) 619–624.
[32] Y. van Kooyk, C.G. Figdor, Avidity regulation of integrins: the driving force in leukocyte adhesion, Curr. Opin. Cell Biol. 12 (2000) 542–547.
[33] B.A. Lollo, K.W. Chan, E.M. Hanson, V.T. Moy, A.A. Brian, Direct evidence for two affinity states for lymphocyte function-associated antigen 1 on activated T cells, J. Biol. Chem. 268 (1993) 21693–21700.
[34] A. Tozeren, L.H. Mackie, M.B. Lawrence, P.Y. Chan, M.L. Dustin, T.A. Springer, Micromanipulation of adhesion of phorbol 12-myristate-13-acetate-stimulated T lymphocytes to planar membranes containing intercellular adhesion molecule-1, Biophys. J. 63 (1992) 247–258.